

15. Franz, M., Kallin, C. & Berlinsky, A.J. Impurity scattering and localization in *d*-wave superconductors *Phys. Rev. B* **54**, R6897–R6900 (1996).
16. Salkola, M.I. & Schrieffer, J.R. Unusual states of inhomogeneous $d_{x^2-y^2} + id_{xy}$ superconductors *Phys. Rev. B* **58**, R5952–R5955 (1998).
17. Atkinson, W.A. & MacDonald, A.H. Visualizing quasiparticle scattering resonances *Science* **285**, 57–58 (1999).
18. Tsuchiura, H., Tanaka, Y., Ogata, M. & Kashiwaya, S. Quasiparticle properties around a nonmagnetic impurity in the superconducting state of the two-dimensional *t*-*J* model. *J. Phys. Soc. Jpn* **68**, 2510–2513 (1999).
19. Flatté, M.E. & Byers, J.M. Local electronic structure of defects in superconductors *Solid State Phys.* **52**, 137–228 (1999).
20. Salkola, M.I., Balatsky, A.V. & Schrieffer, J.R. Spectral properties of quasiparticle excitations induced by magnetic moments in superconductors *Phys. Rev. B* **55**, 12648–12661 (1997).
21. Crommie, M.F., Lutz, C.P. & Eigler, D.M. Imaging standing waves in a two-dimensional gas *Nature* **363**, 524–527 (1993).
22. Zheng, J.F. *et al.* Scanning tunneling microscopy studies of Si donors (Si_{Ga}) in GaAs. *Phys. Rev. Lett.* **72**, 1490–1493 (1994).
23. Yazdani, A., Jones, B.A., Lutz, C.P., Crommie, M.F. & Eigler, D.M. Probing the local effects of magnetic impurities on superconductivity *Science* **275**, 1767–1770 (1997).
24. Madhavan, V., Chen, W., Jamneala, T., Crommie, M.F. & Wingreen, N.S. Tunneling into a single magnetic atom: spectroscopic evidence of the Kondo resonance *Science* **280**, 567–569 (1998).
25. Witteven, Chr., Dombrowski, R., Morgenstern, M. & Wiesendanger, R. Scattering states of ionized dopants probed by low temperature scanning tunneling spectroscopy *Phys. Rev. Lett.* **81**, 5616–5619 (1998).
26. Hudson, E.W., Pan, S.H., Gupta, A.K., Ng, K.-W. & Davis, J.C. Atomic-scale quasiparticle scattering resonances in $\text{Bi}_2\text{Sr}_2\text{CaCu}_2\text{O}_{8+\delta}$ *Science* **285**, 88–91 (1999).
27. Yazdani, A., Howald, C.M., Lutz, C.P., Kapitulnik, A. & Eigler, D.M. Impurity-induced bound excitations on the surface of $\text{Bi}_2\text{Sr}_2\text{CaCu}_2\text{O}_8$ *Phys. Rev. Lett.* **83**, 176–179 (1999).
28. Motohira, N., Kuwahara, K., Hasegawa, T., Kishio, K. & Kitazawa, K. Single crystal growth of $\text{Bi}_2\text{Sr}_2\text{Ca}_{1-x}\text{Cu}_x\text{O}_y$ superconductors by the floating zone method *J. Ceram. Soc. Jpn* **97**, 1009–1014 (1989).
29. Wells, B.O. *et al.* Evidence for *k*-dependent, in-plane anisotropy of the superconducting gap in $\text{Bi}_2\text{Sr}_2\text{CaCu}_2\text{O}_{8+\delta}$ *Phys. Rev. B* **46**, 11830–11834 (1992).
30. Andersen, O. K., Jepsen, O., Liechtenstein, A. I. & Mazin, I. I. Plane dimpling and saddle-point bifurcation in the band structures of optimally doped high-temperature superconductors: a tight-binding model. *Phys. Rev. B* **49**, 4145–4157 (1994).
31. Mahajan, A.V., Alloul, H., Collin, G. & Marucco, J.F. ^{89}Y NMR probe of Zn induced local moments in $\text{YBa}_2(\text{Cu}_{1-y}\text{Zn}_y)_3\text{O}_{6-x}$ *Phys. Rev. Lett.* **72**, 3100–3103 (1994).
32. Nagaosa, N. & Lee, P.A. Kondo effect in high- T_c cuprates. *Phys. Rev. Lett.* **79**, 3755–3758 (1997).

Acknowledgements

We thank A. Balatsky, D. Bonn, M. Crommie, M. Flatté, M. Franz, S. Kashiwaya, A. de Lozanne, A. MacDonald, V. Madhavan, M. Ogata, J. Orenstein, D. J. Scalapino, Z.-X. Shen, Y. Tanaka and D. van der Marel for conversations and communications. This work was supported by the LDRD Program of the Lawrence Berkeley National Laboratory under contract to the Department of Energy, by the D. & L. Packard Foundation, by an IBM predoctoral fellowship (K.M.L.), by Grant-in-Aid for Scientific Research on Priority Area (Japan), and by a COE grant from the Ministry of Education, Japan.

Correspondence and requests for materials should be addressed to J.C.D. (e-mail: jcdavis@socrates.berkeley.edu).

High-efficiency fluorescent organic light-emitting devices using a phosphorescent sensitizer

M. A. Baldo*, M. E. Thompson† & S. R. Forrest*

* Center for Photonics and Optoelectronic Materials (POEM), Department of Electrical Engineering and the Princeton Materials Institute, Princeton University, Princeton, New Jersey 08544, USA

† Department of Chemistry, University of Southern California, Los Angeles, California 90089, USA

To obtain the maximum luminous efficiency from an organic material, it is necessary to harness both the spin-symmetric and anti-symmetric molecular excitations (bound electron-hole pairs, or excitons) that result from electrical pumping. This is possible if the material is phosphorescent, and high efficiencies have been observed in phosphorescent^{1,2} organic light-emitting devices³. However, phosphorescence in organic molecules is rare at room temperature. The alternative radiative process of fluor-

escence is more common, but it is approximately 75% less efficient, due to the requirement of spin-symmetry conservation⁴. Here, we demonstrate that this deficiency can be overcome by using a phosphorescent sensitizer to excite a fluorescent dye. The mechanism for energetic coupling between phosphorescent and fluorescent molecular species is a long-range, non-radiative energy transfer: the internal efficiency of fluorescence can be as high as 100%. As an example, we use this approach to nearly quadruple the efficiency of a fluorescent red organic light-emitting device.

Light is generated in organic materials from the decay of molecular excited states, also known as excitons. Understanding the properties and interactions of excitons is crucial to the design of efficient organic devices for use in displays, lasers and other illumination applications. For example, the spin-symmetry of an exciton determines its probability of radiative recombination and also its multiplicity. Spin-symmetric excitons with a total spin of $S = 1$ have a multiplicity of three and are known as triplets. Spin-antisymmetric excitons ($S = 0$) have a multiplicity of one and are known as singlets. During electrical excitation approximately one singlet exciton is created for every three triplet excitons⁴, but because the ground state is typically also spin-antisymmetric, only relaxations of singlet excitons conserve spin and generate fluorescence. Usually the energy in triplet excitons is wasted; however, given some perturbation in symmetry, triplets may slowly radiatively decay, producing the delayed luminescence known as phosphorescence. Although it is often inefficient, phosphorescence may be enhanced if spin-orbit coupling mixes the singlet and triplet states, an effect often promoted by the presence of a heavy metal atom⁵. Indeed, phosphorescent dyes with these properties have demonstrated very high-efficiency electroluminescence^{1,2}.

Very few organic materials have been found to be capable of efficient room-temperature phosphorescence from triplets^{1,2,6}. In contrast, many organic molecules exhibit fluorescence^{7,8} and fluorescence is also unaffected by triplet-triplet annihilation, which degrades phosphorescent emission efficiency at high excitation densities¹. Consequently, fluorescent materials are suited to many electroluminescent applications, particularly those such as passive matrix displays that require high excitation densities.

It is desirable therefore to find a process whereby triplets that are formed after electrical excitation are not wasted, but are instead transferred to the singlet excited state of a fluorescent dye. There are two mechanisms for triplet-singlet energy transfer from a donor molecule (D) to an acceptor (A). In Dexter transport⁵, the exciton hops directly between molecules. This is a short-range process dependent on the overlap of molecular orbitals of neighbouring molecules. It also preserves the symmetry of the donor and acceptor pair⁵. Thus, a triplet-singlet energy transfer is not possible by a Dexter mechanism. A change in spin-symmetry is possible if the donor exciton breaks up and reforms on the acceptor by incoherent electron exchange⁵. However, this process is considered to be relatively unlikely as it requires the dissociation of the donor exciton, which in most molecular systems has a binding energy of ~ 1 eV.

The alternative mechanism is Förster energy transfer⁵. Here, molecular transition dipoles couple and exchange energy. The efficiency of energy transfer (η_{ET}) is:

$$\eta_{\text{ET}} = \frac{k_{\text{ET}}}{k_{\text{ET}} + k_{\text{r}} + k_{\text{nr}}} \tag{1}$$

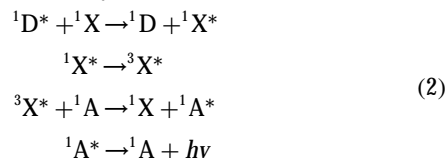
Here k_{ET} is the rate of Förster energy transfer from D to A and k_{r} and k_{nr} are the radiative and non-radiative rates on the donor, respectively. From equation (1), energy transfer is efficient if $k_{\text{ET}} \gg k_{\text{r}} + k_{\text{nr}}$; however, in Förster's theory k_{ET} is proportional to the oscillator strength of the donor transition⁵, as is k_{r} . Thus, η_{ET} is approximately independent of oscillator strength if $k_{\text{r}} \gg k_{\text{nr}}$, that is, if the donor is efficiently phosphorescent then it is possible to

obtain triplet–singlet energy transfer by the Förster mechanism. We note that a ‘pure’ triplet has an infinite lifetime and no probability of Förster energy transfer because the oscillator strength of its decay is zero. However, the slightest perturbation (that is, some overlap between the triplet and ground state on the donor) can counteract the presence of non-radiative modes and yield efficient energy transfer. Such triplet–singlet energy transfers were predicted by Förster⁹ and confirmed by Ermolaev and Sveshnikova¹⁰, who detected the energy transfer using a range of phosphorescent donors and fluorescent acceptors in rigid media at 77 K or 90 K. Large transfer distances were observed; for example with triphenylamine as the donor and chrysoidine as the acceptor, the interaction range is 52 Å.

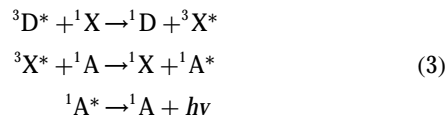
Unfortunately, when a fluorescent acceptor is doped directly into a phosphorescent donor material, the close proximity of the donor and acceptor increases the likelihood of Dexter transfer between the donor and the acceptor triplets. Once excitons reach the acceptor triplet state, they are effectively lost since these fluorescent dyes typically exhibit extremely inefficient phosphorescence (that is, $k_{NR} \gg k_R$).

Another technique is to dope both the phosphorescent material and the fluorescent acceptor into a conductive organic host. Ideally, the phosphor then sensitizes the energy transfer from the host, now acting as the donor, to the fluorescent acceptor. Cascade Förster energy transfer of singlets has been demonstrated for fluorescent materials¹¹; however, here all energy is ideally transferred into the

triplet state of the sensitizer, where it is then transferred to the singlet state of the fluorescent dye, that is:



and



Here, the photon energy is $h\nu$, and the donor, sensitizer and fluorescent acceptor are represented by D, X and A, respectively. Triplet and singlet states are signified by a superscript 3 or 1, respectively, and excited states are marked by asterisks. The multiple-stage energy transfer is described schematically in Fig. 1. Dexter transfers are indicated by dotted arrows and Förster transfers by solid arrows. Processes resulting in a loss in efficiency are marked with a cross. In addition to the energy transfer paths shown in Fig. 1, direct electron–hole recombination is possible on the phosphorescent and fluorescent dopants as well as the host. Triplet exciton formation after charge recombination on the fluorescent dye is another potential loss mechanism.

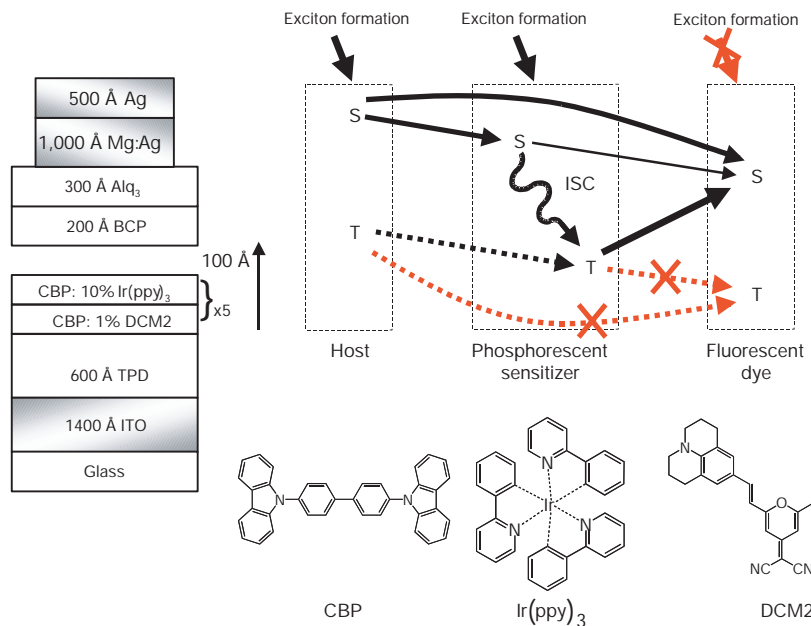


Figure 1 Proposed energy transfer mechanisms in the sensitized system. In principle, all excitons are transferred to the singlet state of the fluorescent dye, as triplets in the dye non-radiatively recombine. Förster transfers are represented by solid lines and Dexter transfers by dotted lines. Electron–hole recombination creates singlet (S) and triplet (T) excitons in the host material, although as indicated, charge trapping may be responsible for exciton formation in the other materials as well. There is a probability of direct transfer into the singlet state of the fluorescent dye by a Förster process, or Dexter transfer into the triplet state. This is a source of loss and is indicated by a cross. Singlet excitons in the phosphor are subject to intersystem crossing (ISC) and transfer to the triplet state. From this state, the triplets may either dipole–dipole couple with the singlet state of the fluorescent dye or, in another loss mechanism, they may Dexter transfer to the triplet state. Direct formation of triplets on the fluorescent dye is an additional path to loss. Inset, the structure of the principal materials and electroluminescent devices fabricated in this work. We use the green emitting phosphor² *fac* tris(2-phenylpyridine) iridium (Ir(ppy)₃) and the red fluorescent dye¹⁷ [2-methyl-6-(2-(2,3,6,7-tetrahydro-1H,5H-benzo[*l*]quinolizin-9-yl) ethenyl)-4H-pyran-4-ylidene] propane-dinitrile (DCM2). DCM2 absorbs in the green

and it emits at wavelengths between $\lambda = 570\text{nm}$ and $\lambda = 650\text{nm}$ (ref. 14). To demonstrate the multiple-stage transfer, we used 4,4'-N,N'-dicarbazole-biphenyl (CBP) as the donor and host material¹⁸. Organic layers were deposited by high vacuum (10^{-6} Torr) thermal evaporation onto a clean glass substrate pre-coated with a layer 1,400 Å in thickness of transparent and conductive indium tin oxide. A layer 600 Å in thickness of N,N'-diphenyl-N,N'-bis(3-methylphenyl)-[1,1'-biphenyl]-4,4'-diamine (TPD) is used for hole transport. We used an alternating series of layers 10 Å in thickness of 10% Ir(ppy)₃/CBP and 1% DCM2/CBP. In total, 10 doped layers were grown with a total thickness of 100 Å. Excitons were confined within the luminescent region by a layer 200 Å in thickness of the wide-energy-gap material 2,9-dimethyl-4,7-diphenyl-1,10-phenanthroline (bathocuproine, or BCP). A layer 300 Å in thickness of tris-(8-hydroxyquinoline) aluminium (Alq₃) is used to transport electrons to the luminescent region and to reduce absorption at the cathode. Metal deposition through a shadow mask with openings 1 mm in diameter defined cathodes consisting of a layer 1000 Å in thickness of 25:1 Mg/Ag, with an Ag cap 500 Å in thickness.

The structure of the organic devices and the principal materials used to demonstrate the sensitized energy transfer are shown in the inset of Fig. 1. We used CBP as the host and exciton donor, the green phosphor Ir(ppy)₃ as the sensitizer and the red fluorescent dye DCM2 as the acceptor. As a control, two other organic light-emitting device (OLED) structures were made. In the first, Ir(ppy)₃ was replaced by Alq₃, which has similar emission and absorption spectra, but no observable phosphorescence at room temperature. From the spectral overlap with DCM2 and the photoluminescent efficiencies^{12,13} of Alq₃ and Ir(ppy)₃, the Förster transfer radii for Alq₃ to DCM2 and Ir(ppy)₃ to DCM2 are both calculated to be ~40 Å (ref. 14). In the second device, the sensitizer was completely omitted in order to examine direct energy transfer from the donor, CBP, to the acceptor, DCM2.

The external quantum efficiency (photons per electron) of the DCM2 portion of the emission spectrum of these three devices is shown as a function of injected current density in Fig. 2. The DCM2 emission efficiency of the device containing the phosphorescent sensitizer is significantly higher than its fluorescent analogue. Indeed, the peak efficiency of (3.3±0.1)% is significantly higher than the best result of ~2% observed for DCM2-based OLEDs in

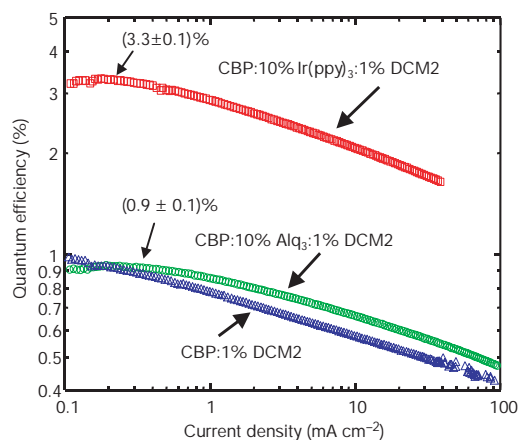


Figure 2 The external quantum efficiencies of DCM2 emission in the three devices. The sensitizing action of Ir(ppy)₃ improves the efficiency. We also note that the presence of Alq₃ in the all-fluorescent devices makes little or no difference. The CBP/10% Ir(ppy)₃/1% DCM2 device reaches a brightness of 100 cd m⁻² at 9.9 V (3 lm W⁻¹).

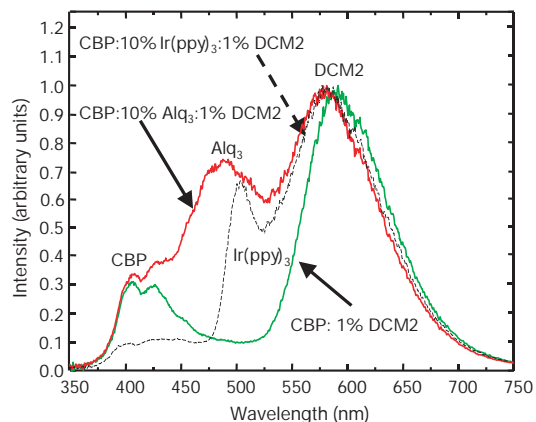


Figure 3 The spectra of the three electroluminescent devices fabricated in this work. Characteristic peaks are observed for CBP (at wavelength $\lambda \approx 400$ nm), TPD ($\lambda \approx 430$ nm), Alq₃ ($\lambda \approx 490$ nm), Ir(ppy)₃ ($\lambda \approx 500$ nm) and DCM2 ($\lambda \approx 590$ nm). Approximately 80% of the photons in the Ir(ppy)₃ device are emitted by DCM2. All spectra were recorded at a current density of ~1 mA cm⁻². Note that the peak intensities of each of the spectra are normalized for comparison.

previous studies¹⁵, suggesting that host triplets are transferred to the fluorescent singlet state. We also note that addition of Alq₃ to the unsensitized CBP/DCM2 device makes no significant difference to the maximum efficiency of (0.9±0.1)% of DCM2 emission.

The emission spectra of the OLEDs are shown in Fig. 3. All devices show energy transfer to the fluorescent dye. By calculating the area under the various spectral peaks, we find that approximately 80% of photons are emitted by DCM2 in the device containing the Ir(ppy)₃ sensitizer. The remainder contribute to CBP luminescence at $\lambda \approx 400$ nm, TPD luminescence at $\lambda \approx 430$ nm and Ir(ppy)₃ luminescence at $\lambda \approx 500$ nm. In the device doped with 10% Alq₃, an emission peak is also observed at $\lambda \approx 490$ nm. This is consistent with earlier observations¹⁶ of Alq₃ emission in a non-polar host such as CBP.

Conclusive evidence of the energy transfer of equations (2) and (3) is provided by examining the transient behaviour of the DCM2 and Ir(ppy)₃ components of the emission spectra. These data are shown in Fig. 4, and were obtained by applying a ~100 ns electrical pulse to the electroluminescent device. The resulting emission was measured using a streak camera. If a fraction of the DCM2 emission originates by transfer from Ir(ppy)₃ triplets, then the proposed energy transfer must yield delayed DCM2 fluorescence. Furthermore, since the radiative lifetime of DCM2 is much shorter than that of Ir(ppy)₃, the transient decay of DCM2 should match that of Ir(ppy)₃. After an initial peak, most probably due to CBP/DCM2 singlet-singlet transfer and exciton formation on DCM2, the DCM2 decay does indeed trace the Ir(ppy)₃ decay. The transient lifetime of Ir(ppy)₃ in this system is ~100 ns, compared to a lifetime of ~500 ns in the absence of DCM2. Since these lifetimes are inversely proportional to the rates of exciton transfer and relaxation, respectively, this confirms an energy transfer of ~80%. The decrease in the triplet lifetime as a result of energy transfer to the fluorescent acceptor is advantageous. Not only does it increase the transient response of the system, but it should also reduce the probability of triplet-triplet annihilation. Thus, it is expected that this multi-stage energy transfer will reduce the quenching of triplet states, thereby further enhancing the potential efficiency of sensitized fluorescence.

The transient response of the sensitized system may be further examined to determine the relative efficiencies of the singlet-to-singlet and triplet-to-singlet energy transfer pathways. By subtracting

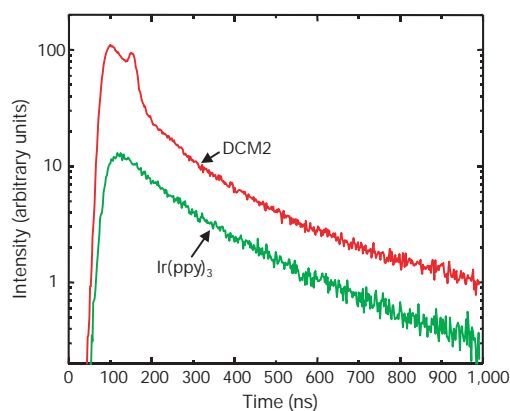


Figure 4 The transient response of the DCM2 and Ir(ppy)₃ spectral components in the CBP/10% Ir(ppy)₃/1% DCM2 device. The transient lifetime of DCM2 is ~1 ns, thus in the case of energy transfer from Ir(ppy)₃, the response of DCM2 should be governed by the transient lifetime of Ir(ppy)₃. After the initial 100-ns-wide electrical excitation pulse, this is clearly the case, demonstrating that energy is transferred from the triplet state in Ir(ppy)₃ to the singlet state in DCM2. However, during the excitation pulse, singlet transfer to DCM2 is observed, resulting in the ripples in the transient response. These ripples are due to fluctuations in the current density and the discharge of traps at the falling edge of the pulse. We note that the trends in the DCM2 and Ir(ppy)₃ transient responses eventually diverge. This is caused by charge trapped on DCM2 molecules recombining and causing luminescence.

the transient decay of Ir(ppy)₃ from the DCM2 transient, the ratio of instantaneous to delayed DCM2 fluorescence is found to be ~ 1:2. Consequently, we expect that the sensitized OLED should have a quantum efficiency roughly triple that of an OLED that does not exhibit delayed fluorescence. Indeed, from the data in Fig. 2, the improvement in peak quantum efficiencies is (3.7 ± 0.5)%. Ideally the ratio of singlets to triplets (1:3), or even be weighted towards triplets if intersystem crossing on Ir(ppy)₃ is significant. It is likely that direct triplet exciton formation on DCM2 contributes to some loss. In addition, the likelihood of triplet transfer from CBP to DCM2, CBP to Ir(ppy)₃, or even Ir(ppy)₃ to CBP is unknown, so it is possible that some triplets are transferred directly to DCM2, bypassing the sensitizer.

In conclusion, we have demonstrated a general technique for improving the efficiency of fluorescence in OLEDs. Further improvement in energy transfer efficiency could be expected by mixing the host, phosphorescent sensitizer and fluorescent dye rather than doping in alternating thin layers as was done here. However, a mixture may possess increased losses from Dexter transfer from the sensitizer to the triplet state of the fluorescent dye. To reduce this loss, an ideal system may incorporate low concentrations of a sterically hindered fluorescent dye. For example, adding spacer groups to the DCM2 molecule could decrease the probability of Dexter transfer to the dye while minimally affecting its participation in Förster transfer or its luminescence efficiency. As Dexter transfer can be understood as the simultaneous transfer of an electron and a hole, steric hindrance may also reduce the likelihood of charge trapping on the fluorescent dye. Similar efforts have already reduced non-radiative excimer formation in a DCM2 variant¹⁵. M

Received 19 July; accepted 20 December 1999.

- Baldo, M. A. *et al.* Highly efficient phosphorescent emission from organic electroluminescent devices. *Nature* **395**, 151–154 (1998).
- Baldo, M. A., Lamansky, S., Burrows, P. E., Thompson, M. E. & Forrest, S. R. Very high-efficiency green organic light-emitting devices based on electrophosphorescence. *Appl. Phys. Lett.* **75**, 4–6 (1999).
- VanSlyke, S. A. & Tang, C. W. Organic electroluminescent devices having improved power conversion efficiencies. (US Patent No. 4539507, 1985).
- Baldo, M. A., O'Brien, D. F., Thompson, M. E. & Forrest, S. R. The excitonic singlet-triplet ratio in a semiconducting organic thin film. *Phys. Rev. B* **60**, 14422–14428 (1999).
- Klessinger, M. & Michl, J. *Excited States and Photochemistry of Organic Molecules* (VCH Publishers, New York, 1995).
- Cleave, V., Yahioğlu, G., Le Barny, P., Friend, R. & Tessler, N. Harvesting singlet and triplet energy in polymer LEDs. *Adv. Mater.* **11**, 285–288 (1999).
- Chen, C. H., Shi, J. & Tang, C. W. Recent developments in molecular organic electroluminescent materials. *Macromol. Symp.* **125**, 1–48 (1997).
- Brackmann, U. *Lambdachrome Laser Dyes* (Lambda Physik, Göttingen, 1997).
- Forster, T. Transfer mechanisms of electronic excitation. *Discuss. Faraday Soc.* **27**, 7–17 (1959).
- Ermolaev, V. L. & Sveshnikova, E. B. Inductive-resonance transfer of energy from aromatic molecules in the triplet state. *Dokl. Akad. Nauk* **149**, 1295–1298 (1963).
- Berggren, M., Dodabalapur, A., Slusher, R. E. & Bao, Z. Light amplification in organic thin films using cascade energy transfer. *Nature* **389**, 466–469 (1997).
- Garbuzov, D. Z., Bulovic, V., Burrows, P. E. & Forrest, S. R. Photoluminescence efficiency and absorption of aluminium-tris-quinolate (Alq₃) thin films. *Chem. Phys. Lett.* **249**, 433–437 (1996).
- Vander Donckt, E., Camerman, B., Hendrick, F., Herne, R. & Vandeloise, R. Polystyrene immobilized Ir(III) complex as a new material for oxygen sensing. *Bull. Soc. Chim. Belg.* **103**, 207–211 (1994).
- Bulovic, V. *et al.* Bright, saturated, red-to-yellow organic light-emitting devices based on polarization-induced spectral shifts. *Chem. Phys. Lett.* **287**, 455–460 (1998).
- Chen, C. H., Tang, C. W., Shi, J. & Klubeck, K. P. Improved red dopants for organic electroluminescent devices. *Macromol. Symp.* **125**, 49–58 (1997).
- Bulovic, V., Deshpande, R., Thompson, M. E. & Forrest, S. R. Tuning the color emission of thin film molecular organic light emitting devices by the solid state solvation effect. *Chem. Phys. Lett.* **308**, 317 (1999).
- Tang, C. W., VanSlyke, S. A. & Chen, C. H. Electroluminescence of doped organic thin films. *J. Appl. Phys.* **65**, 3610–3616 (1989).
- O'Brien, D. F., Baldo, M. A., Thompson, M. E. & Forrest, S. R. Improved energy transfer in electrophosphorescent devices. *Appl. Phys. Lett.* **74**, 442–444 (1999).

Acknowledgements

This work was supported by Universal Display Corporation, the Defense Advanced Research Projects Agency, the Air Force Office of Scientific Research and the National Science Foundation.

Correspondence and requests for materials should be addressed to S.R.F. (e-mail: forrest@ee.princeton.edu).

.....
Explanation for fracture spacing in layered materials

T. Bai*, D. D. Pollard* & H. Gao†

* Department of Geological and Environmental Sciences,
† Department of Mechanical Engineering, Stanford University,
Stanford, California 94305-2115, USA

.....
The spacing of opening-mode fractures in layered materials—such as certain sedimentary rocks and laminated engineering materials—is often proportional to the thickness of the fractured layer^{1–4}. Experimental studies of this phenomenon^{1,5} show that the spacing initially decreases as extensional strain increases in the direction perpendicular to the fractures. But at a certain ratio of spacing to layer thickness, no new fractures form and the additional strain is accommodated by further opening of existing fractures: the spacing then simply scales with layer thickness, which is called fracture saturation^{5,6}. This is in marked contrast to existing theories of fracture, such as the stress-transfer theory^{7,8}, which predict that spacing should decrease with increasing strain *ad infinitum*. Recently^{9,10}, two of us (T.B. and D.D.P.) have used a combination of numerical simulations and laboratory experiments to show that, with increasing applied stress, the normal stress acting between such fractures undergoes a transition from tensile to compressive, suggesting a cause for fracture saturation. Here we investigate the full stress distribution between such fractures, from which we derive an intuitive physical model of the process of fracture saturation. Such a model should find wide applicability, from geosciences^{11–13,14} to engineering^{1,2,6,15,16}.

Spacing of opening-mode fractures in layered materials is important to engineers and geoscientists. Mechanical engineers, civil engineers and materials scientists have studied the spacing of fractures in composite materials for structural safety and service life^{1,2,6,15,16}. Geoscientists have investigated fracture density in layered rocks because of its impact on the flow of groundwater and hydrocarbons^{11–13}, and the safety of mines¹⁴. Experimental results using

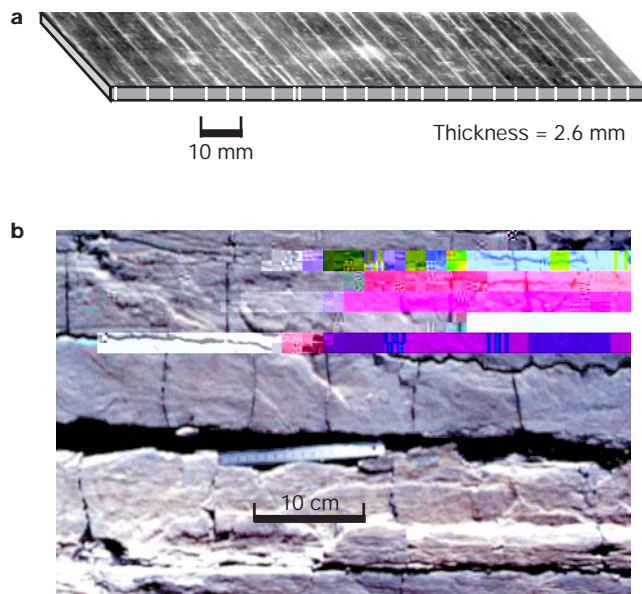


Figure 1 Examples of opening-mode fractures in layered materials. **a**, In a glass-fibre-reinforced polyester (modified from ref. 1). **b**, In the limestone layers of the Carmel Formation, Chimney Rock, Utah.